some of the experiments on $Cp^*_2VCl_2$, and the Natural Sciences and Engineering Research Council of Canada and the donors of the Petroleum Research Fund, administered by the American Chemical Society, for financial support of this work.

Registry No. I, 104090-36-0; II, 104090-37-1; III, 104090-38-2; $Cp^*_2VCl_2$, 83617-50-9; Cp^*VCl_3, 104090-39-3; $Cp^*_2VI_2$, 89710-29-2; $[Cp^*_2V(NO)]_2I_8$, 104090-40-6; $[Cp^*VI(O)]_2(\mu\text{-o})$, 104090-41-7.

Supplementary Material Available: Drawings of I–III and tables of atomic coordinates of the hydrogen atoms, thermal parameters, comprehensive bond distances and angles, and some mean planes for I–III (17 pages); tables of $|F_o|$ and $|F_c|$ for I–III (17 pages). Ordering information is given on any current masthead page.

Alkyne Adducts of Mixed Chloro–Dimethylamido Ditungsten Compounds

Kazi J. Ahmed, Malcolm H. Chisholm,* K. Folting, and J. C. Huffman

Department of Chemistry and Molecular Structure Center, Indiana University, Bloomington, Indiana 47405

Received December 30, 1985

Alkyne adducts of formula $W_2Cl_2(NMe_2)_4(\mu\text{-}C_2RR')(py)_2$ (R = R′ = H; R = R′ = Me; R = Me, R′ = H; R = Ph, R′ = H) have been isolated from the reactions of alkynes with $W_2Cl_2(NMe_2)_4$ in the presence of pyridine. These compounds, with the exception of $W_2Cl_2(NMe_2)_4(\mu\text{-}C_2H_2)(py)_2$ (III), undergo thermal ligand redistribution reactions in hydrocarbon solvents to produce compounds having the general formula $W_2Cl_x(NMe_2)_{6-x}(\mu\text{-alkyne})(py)_2$, where x = 3 and 4, and $W_2(NMe_2)_6$. Thus, $W_2Cl_2(NMe_2)_4(\mu\text{-}PhC_2H)(py)_2$ reacts in toluene at ca. 50 °C to produce $W_2Cl_3(NMe_2)_3(\mu\text{-}PhC_2H)(py)_2 \cdot {}^1/_2C_7H_8$ (V) in good yields. Compound V is very sparingly soluble in hydrocarbon solvents, and no further decomposition has been observed. By contrast, $W_2Cl_2(NMe_2)_4(\mu\text{-}C_2Me_2)(py)_2$ undergoes ligand redistribution in toluene and, at ca. 55 °C, yields $W_2Cl_4(NMe_2)_2(\mu\text{-}C_2Me_2)(py)_2$ (VI) presumably via the initial formation of $W_2Cl_3(NMe_2)_3(\mu\text{-}C_2Me_2)(py)_2$. No further decomposition of compound VI has been observed. Single-crystal X-ray studies reveal pseudotetrahedral $W_2(\mu\text{-}C_2)$ cores in both III and V, arising from the "perpendicular" addition of the alkynes to the $(W{\equiv}W)^{6+}$ centers. The C–C (1.38 (1) Å in III, 1.40 (1) Å in V) and the W–W (2.597 (1) Å in III, 2.657 (1) Å in V) distances approach C–C and W–W single bond distances and conform closely to the description of dimetallatetrahedranes. The overall geometry around each of the tungsten atoms, in III and V, can be considered pseudooctahedral, and these octahedra are joined together through the agency of the $\mu\text{-}C_2H_2$ and two $\mu\text{-}NMe_2$ ligands in III and by the ligands $\mu\text{-}PhC_2H$ and μ-Cl and one $\mu\text{-}NMe_2$ in V. Compound VI, on the other hand, contains a $\mu\text{-}C_2Me_2$ moiety which shows a large deviation, θ = 35°, from being in an ideal perpendicular orientation, θ = 0. There are two significantly different W–C distances, 2.02 (1) and 2.44 (1) Å, approaching W–C double and nonbonding distances, respectively. These data, coupled with the observed short W–W distance of 2.436 (1) Å, indicate incipient 1,2-dimetallacyclobutadiene characteristics within the $W_2(\mu\text{-}C_2)$ core in VI. These studies are compared with the related alkyne adducts of $W_2(OR)_6$ compounds. Crystal data for (i) $W_2Cl_2(NMe_2)_4(\mu\text{-}C_2H_2)(py)_2 \cdot CH_2Cl_2$ at −160 °C: a = 17.123 (5) Å, b = 12.012 (3) Å, c = 7.410 (1) Å, α = 105.80 (1)°, β = 94.71 (1)°, γ = 101.93 (1)°, Z = 2, d_{calcd} = 2.069 g cm^{-3}, and space group $P\bar{1}$. (ii) $W_2Cl_3(NMe_2)_3(\mu\text{-}PhC_2H)(py)_2 \cdot {}^1/_2C_7H_8$ at −161 °C: a = 14.701 (7) Å, b = 12.137 (6) Å, c = 17.632 (9) Å, β = 103.15 (3)°, Z = 4, d_{calcd} = 1.979 g cm^{-3}, and space group $P2_1/n$. (iii) $W_2Cl_4(NMe_2)_2(\mu\text{-}C_2Me_2)(py)_2$ at −160 °C: a = 10.918 (4) Å, b = 13.440 (5) Å, c = 16.558 (7) Å, β = 104.45 (2)°, Z = 4, d_{calcd} = 2.287 g cm^{-3}, and space group $P2_1/n$.

Introduction

Recent interest in the study of the reactivity between alkynes and ditungsten hexaalkoxides has resulted in a fascinating array of novel organometallic compounds.[1] The products depend on the specific substituents on the alkoxide and the alkyne ligands and also on the reaction conditions. In all, three general reaction types are observed which are summarized in eq 1–3.

$$W_2(OR)_6 + py + R'C{\equiv}CR \quad (1)$$

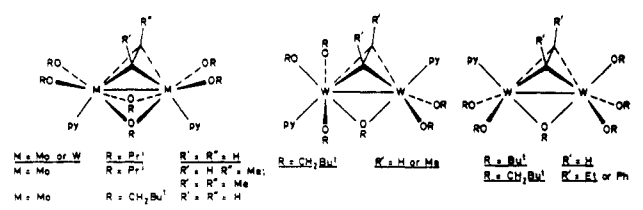

$$W_2(O\text{-}t\text{-}Bu)_6 + RC{\equiv}CR \rightarrow 2(Bu\text{-}t\text{-}O)_3W{\equiv}CR \quad (2)$$

R = Me, Et, Pr, etc (see *Organometallics* **1985**, *4*, 69)

$$W_2(O\text{-}t\text{-}Bu)_6 + 2C_2H_2 \rightarrow W_2(O\text{-}t\text{-}Bu)_6(\mu\text{-}C_4H_4) \quad (3a)$$

$$W_2(OR)_6 + 3R'C{\equiv}CR' \rightarrow W_2(OR)_6(\mu\text{-}C_4R_4')(C_2R_2') \quad (3b)$$

R = *i*-Pr, CH_2-*t*-Bu; R′ = H, Me

It is clearly evident that the steric bulk of the alkoxide ligands as well as the substituents on the alkynes play a major role in determining the nature of the products.

With this background, attention was turned to reactions of alkynes with $(W{\equiv}W)^{6+}$ centers containing other ligands. It has been observed that $W_2(NMe_2)_6$ does not react with alkynes.[2] However, substitution of two NMe_2 ligands by

(1) Chisholm, M. H.; Hoffman, D. M.; Huffman, J. C. *Chem. Soc. Rev.* **1985**, *14*, 69.
(2) Ahmed, K. J.; Chisholm, M. H., unpublished work.

0276-7333/86/2305-2171$01.50/0

Cl ligands greatly enhances the reactivity (electrophilicity) of the ditungsten center. Moreover, the NMe_2 group is as good, if not better, a π-donor as are alkoxide ligands. Therefore, similarity (or dissimilarity) of reactivities of alkynes toward $W_2(OR)_6$ and $W_2Cl_2(NMe_2)_4$ compounds would provide further insight into the chemistry of the alkyne adducts of $(W{\equiv}W)^{6+}$ centers.

Results and Discussion

Synthesis. Addition of alkynes to toluene solutions of $W_2Cl_2(NMe_2)_4$, in the presence of pyridine, results in rapid reactions and produces compounds of formula $W_2Cl_2(NMe_2)_2(\mu\text{-}NMe_2)_2(\mu\text{-alkyne})(py)_2$ according to eq 4. The

$$W_2Cl_2(NMe_2)_4 + py + RC{\equiv}CR' \xrightarrow{\text{toluene}} W_2Cl_2(NMe_2)_2(\mu\text{-}NMe_2)_2(\mu\text{-}C_2RR')(py)_2 \quad (4)$$

R = Me(I), Ph(II), R′ = H; R = R′ = H(III), Me(IV)

rates of the reactions follow the order PhC≡CH ($t_{1/2}$ = ca. 5 min) > HC≡CH ($t_{1/2}$ = ca. 15 min) > MeC≡CH ($t_{1/2}$ = ca. 45 min) > MeC≡CMe ($t_{1/2}$ = ca. 2 h), suggesting a rate dependence on steric as well as electronic factors associated with the alkynes.

Compounds I, II, III, and IV precipitate from the reaction medium as microcrystalline solids and can be isolated by filtration. The complexes are very sensitive to oxygen and moisture. With the exception of III, all the alkyne adducts are thermally unstable and disproportionate rapidly in solution to produce $W_2Cl_3(NMe_2)_3(C_2R_2)(py)_2$ and $W_2Cl_4(NMe_2)_2(C_2R_2)(py)_2$ compounds according to eq 5 and 6. Compounds V and VI are isolable

$$3W_2Cl_2(NMe_2)_4(C_2RR')(py)_2 \xrightarrow[\text{toluene}]{50\ ^\circ C} 2\underset{\text{V}}{W_2Cl_3(NMe_2)_3(C_2RR')(py)_2} + W_2(NMe_2)_6 + 2py + RC{\equiv}CR' \quad (5)$$

R = Ph, R′ = H

$$2W_2Cl_2(NMe_2)_4(C_2RR')(py)_2 \xrightarrow[\text{toluene}]{55\ ^\circ C} \underset{\text{VI}}{W_2Cl_4(NMe_2)_2(C_2RR')(py)_2} + W_2(NMe_2)_6 + 2py + RC{\equiv}CR' \quad (6)$$

R = R′ = Me

crystalline materials which are fairly air-sensitive, although no sign of decomposition, over a period of months, was observed when stored under dinitrogen or when stored in sealed ampules under vacuum.

The ligand redistribution reactions 5 and 6 are very similar to the observed Cl for NMe_2 redistribution reactions involving $W_2Cl_2(NMe_2)_4L_2$ and $W_2Cl_3(NMe_2)_3L_2$ (L = PMe_3, PMe_2Ph) compounds.[3] Although no intermediate $W_2Cl_3(NMe_2)_3(C_2Me_2)(py)_2$ could be isolated during the thermal decomposition of $W_2Cl_2(NMe_2)_4(C_2Me_2)(py)_2$ to produce compound VI, it is, by all means, a very viable intermediate, which then can react further according to the stoichiometry shown in eq 7. The reason for the lack

$$4W_2Cl_3(NMe_2)_3(C_2Me_2)(py)_2 \xrightarrow{\Delta} 3VI + W_2(NMe_2)_6 + MeC{\equiv}CMe + 2\ py \quad (7)$$

of any further decomposition of $W_2Cl_3(NMe_2)_3(PhC_2H)(py)_2$ (V) can best be ascribed to its insolubility in hydrocarbon solvents. The compound is soluble in coordinating solvents, e.g., THF and pyridine, although no thermal decomposition has been observed even after 1 week at 60 °C.

Compounds I–VI have been characterized by NMR spectroscopy, and, in particular, compounds III, V, and VI have also been studied by single-crystal X-ray analysis. Analytical data, IR data, and ^1H and ^{13}C NMR data are given in the Experimental Section.

Solid-State Structural Considerations. Atomic positional parameters are given in Tables I–III and selected bond distances and angles for $W_2Cl_2(NMe_2)_4(\mu\text{-}C_2H_2)(py)_2{\cdot}CH_2Cl_2$, $W_2Cl_3(NMe_2)_3(\mu\text{-}PhC_2H)(py)_2{\cdot}{}^1/_2C_7H_8$, and

Table I. Fractional Coordinates and Isotropic Thermal Parameters for $W_2(NMe_2)_4Cl_2(py)_2(\mu\text{-}C_2H_2)\cdot CH_2Cl_2$

atom	10^4x	10^4y	10^4z	$10B_{iso}$, Å^2
W(1)	2453.1 (2)	2513.6 (2)	1214.9 (4)	9
W(2)	3095.2 (2)	691.2 (2)	454.4 (4)	9
Cl(3)	2209 (1)	3650 (2)	−1057 (3)	14
Cl(4)	3421 (1)	−275 (2)	−2726 (3)	15
C(5)	2382 (5)	1093 (7)	2520 (11)	13
C(6)	3081 (4)	1978 (7)	3140 (11)	11
N(7)	1475 (4)	2833 (5)	2346 (9)	15
C(8)	1299 (5)	4024 (7)	2739 (12)	16
C(9)	918 (5)	2123 (8)	3199 (13)	18
N(10)	3087 (4)	4349 (5)	3152 (8)	11
C(11)	3475 (5)	5235 (7)	2588 (12)	16
C(12)	3809 (5)	6377 (7)	3796 (12)	19
C(13)	3719 (5)	6612 (8)	5686 (12)	22
C(14)	3324 (5)	5705 (7)	6311 (12)	18
C(15)	3018 (5)	4598 (7)	5024 (12)	15
N(16)	1941 (4)	896 (5)	−1088 (9)	14
C(17)	1166 (5)	136 (7)	−872 (12)	17
C(18)	1847 (5)	879 (7)	−3058 (11)	16
N(19)	3654 (4)	2410 (5)	118 (9)	12
C(20)	3824 (5)	2539 (8)	−1721 (12)	16
C(21)	4403 (5)	3105 (7)	1443 (11)	15
N(22)	4002 (4)	261 (5)	1728 (9)	13
C(23)	4503 (5)	882 (8)	3573 (12)	18
C(24)	4235 (5)	−875 (8)	1005 (12)	17
N(25)	2430 (4)	−1191 (5)	167 (9)	14
C(26)	2030 (5)	−1979 (8)	−1507 (13)	20
C(27)	1649 (5)	−3143 (7)	−1638 (12)	22
C(28)	1669 (5)	−3537 (8)	−59 (13)	23
C(29)	2068 (5)	−2733 (8)	1652 (14)	21
C(30)	2429 (5)	−1589 (7)	1703 (13)	18
Cl(31)	10439 (1)	8659 (2)	3530 (3)	25
C(32)	9952 (5)	7269 (9)	1933 (13)	25
Cl(33)	10071 (1)	6084 (2)	2843 (4)	36

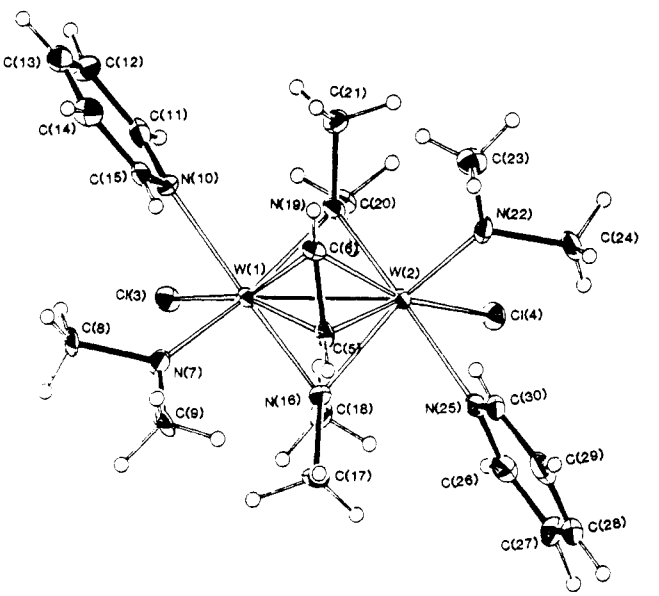

Figure 1. An ORTEP view of the $W_2Cl_2(NMe_2)_4(\mu\text{-}C_2H_2)(py)_2$ molecule looking down the virtual C_2 axis showing the atom number scheme used in the tables.

(3) Ahmed, K. J.; Chisholm, M. H.; Folting, K.; Huffman, J. C. *Inorg. Chem.* **1985**, *24*, 4039.

Table II. Fractional Coordinates and Isotropic Thermal Parameters for $W_2Cl_3(NMe_2)_3(py)_2(\mu\text{-PhCCH})\cdot{}^1/_2C_7H_8$

atom	10^4x	10^4y	10^4z	$10B_{iso}$, Å^2
W(1)	9076.0 (4)	561.4 (4)	2218.9 (3)	13
W(2)	10873.9 (4)	667.2 (4)	2192.1 (3)	12
Cl(3)	8003 (2)	-1043 (3)	1816 (2)	18
Cl(4)	9650 (2)	56 (3)	1027 (2)	17
Cl(5)	11818 (2)	-798 (3)	1758 (2)	20
C(6)	10153 (9)	1534 (10)	2893 (7)	14
C(7)	9903 (9)	1951 (10)	2131 (8)	14
C(8)	9772 (8)	3094 (11)	1782 (8)	15
C(9)	9952 (9)	4019 (11)	2252 (8)	16
C(10)	9835 (10)	5078 (11)	1937 (10)	26
C(11)	9561 (10)	5178 (12)	1124 (11)	30
C(12)	9393 (10)	4252 (14)	652 (10)	31
C(13)	9469 (9)	3211 (11)	980 (8)	19
N(14)	11985 (7)	1103 (9)	2976 (7)	20
C(15)	12102 (10)	1536 (12)	3770 (9)	25
C(16)	12924 (9)	1081 (11)	2823 (8)	18
N(17)	7945 (7)	1479 (8)	1415 (7)	16
C(18)	7547 (9)	1135 (12)	689 (8)	18
C(19)	6825 (10)	1678 (12)	210 (8)	24
C(20)	6497 (10)	2654 (13)	478 (9)	25
C(21)	6903 (9)	3036 (12)	1214 (9)	22
C(22)	7617 (9)	2439 (12)	1651 (9)	22
N(23)	8410 (7)	884 (9)	3061 (6)	16
C(24)	8734 (11)	1299 (13)	3835 (9)	28
C(25)	7401 (10)	752 (12)	2918 (9)	23
N(26)	11427 (7)	1716 (9)	1365 (6)	13
C(27)	11409 (9)	1411 (11)	627 (8)	15
C(28)	11693 (10)	2100 (12)	103 (8)	24
C(29)	12080 (8)	3129 (10)	370 (8)	16
C(30)	12106 (9)	3439 (10)	1122 (8)	17
C(31)	11779 (8)	2719 (11)	1606 (10)	24
N(32)	10169 (7)	-617 (9)	2731 (6)	13
C(33)	10130 (10)	-1769 (11)	2414 (9)	23
C(34)	10421 (10)	-705 (12)	3571 (8)	23
C(35)	9538 (17)	4706 (21)	4353 (16)	3 (4)
C(36)	9122 (26)	3899 (33)	5034 (24)	43 (8)
C(37)	9472 (24)	4006 (29)	5828 (21)	102 (9)
C(38)	9729 (35)	5229 (46)	4045 (31)	63 (11)
C(39)	9305 (25)	4445 (31)	4604 (23)	31 (7)
C(40)	10258 (25)	5385 (30)	4664 (22)	38 (7)

Table III. Fractional Coordinates and Isotropic Thermal Parameters for $W_2Cl_4(NMe_2)_4(py)_2(\mu\text{-MeCCMe})$

atom	10^4x	10^4y	10^4z	$10B_{iso}$, Å^2
W(1)	5815.4 (4)	1822.6 (4)	2361.6 (3)	10
W(2)	4249.4 (4)	1837.7 (4)	3183.1 (3)	10
Cl(3)	7872 (3)	2570 (2)	2692 (2)	16
Cl(4)	6685 (3)	325 (2)	1928 (2)	19
Cl(5)	2111 (3)	2430 (3)	2779 (2)	18
Cl(6)	3565 (3)	369 (2)	3790 (2)	17
C(7)	4179 (13)	3911 (11)	1703 (8)	24
C(8)	4822 (11)	3102 (8)	2286 (7)	12
C(9)	5112 (11)	3163 (9)	3140 (7)	12
C(10)	5640 (12)	4056 (10)	3645 (8)	19
N(11)	3947 (9)	1132 (7)	1976 (6)	13
C(12)	3772 (12)	33 (11)	1918 (9)	25
C(13)	2936 (12)	1544 (10)	1269 (8)	21
N(14)	6190 (8)	1306 (7)	3623 (6)	9
C(15)	7112 (11)	1834 (11)	4301 (7)	16
C(16)	6458 (13)	245 (10)	3799 (8)	21
N(17)	5740 (9)	2205 (8)	1008 (6)	13
C(18)	5220 (11)	1586 (9)	383 (8)	17
C(19)	5116 (11)	1855 (10)	-442 (7)	15
C(20)	5590 (11)	2724 (10)	-639 (7)	18
C(21)	6146 (13)	3326 (11)	19 (9)	27
C(22)	6194 (11)	3062 (9)	815 (8)	15
N(23)	4243 (8)	2420 (8)	4476 (6)	14
C(24)	4732 (11)	1921 (10)	5188 (7)	15
C(25)	4688 (11)	2274 (11)	5946 (8)	18
C(26)	4101 (13)	3142 (10)	6007 (8)	22
C(27)	3548 (12)	3686 (10)	5294 (8)	19
C(28)	3636 (10)	3283 (9)	4546 (7)	12

$W_2Cl_4(NMe_2)_2(\mu\text{-}C_2Me_2)(py)_2$ are given in Tables IV–IX. Ortep views of the three molecules giving the atom number scheme used in the tables are shown in Figures 1–3, respectively.

Table IV. Selected Bond Distances (Å) for the $W_2Cl_2(NMe_2)_4(\mu\text{-}C_2H_2)(py)_2\cdot CH_2Cl_2$ Molecule

A	B	dist
W(1)	W(2)	2.5970 (8)
W(1)	Cl(3)	2.4990 (19)
W(1)	N(7)	1.993 (6)
W(1)	N(10)	2.265 (6)
W(1)	N(16)	2.168 (6)
W(1)	N(19)	2.287 (6)
W(1)	C(5)	2.167 (8)
W(1)	C(6)	2.035 (8)
W(2)	Cl(4)	2.4914 (19)
W(2)	N(16)	2.293 (6)
W(2)	N(19)	2.178 (6)
W(2)	N(22)	1.981 (6)
W(2)	N(25)	2.256 (6)
W(2)	C(5)	2.053 (7)
W(2)	C(6)	2.168 (8)
Cl(31)	C(32)	1.752 (9)
Cl(33)	C(32)	1.772 (10)
N(7)	C(8)	1.481 (10)
N(7)	C(9)	1.446 (10)
N(10)	C(11)	1.320 (10)
N(10)	C(15)	1.358 (10)
N(16)	C(17)	1.495 (10)
N(16)	C(18)	1.450 (10)
N(19)	C(20)	1.459 (10)
N(19)	C(21)	1.486 (10)
N(22)	C(23)	1.467 (10)
N(22)	C(24)	1.474 (10)
N(25)	C(26)	1.363 (11)
N(25)	C(30)	1.349 (11)
C(5)	C(6)	1.375 (11)
C–C(pyridine ring)[a]		1.380 (12)

[a] Average.

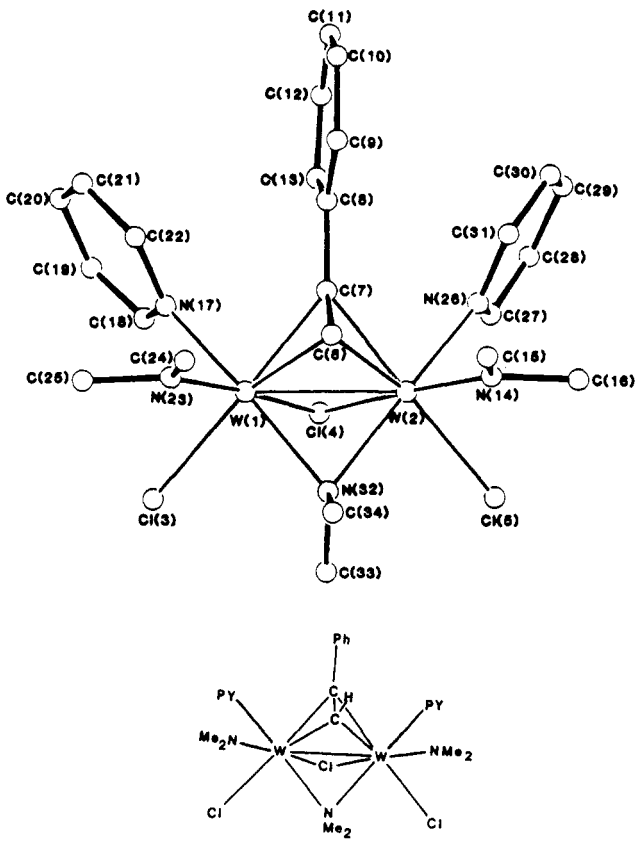

Figure 2. A ball and stick drawing of the $W_2Cl_3(NMe_2)_3(\mu\text{-}PhC_2H)(py)_2$ molecule showing the numbering scheme used for the atoms. The molecule has a virtual mirror plane containing the bridging ligand atoms C(7), C(8), Cl(4) and N(32), C(33), C(34).

Table V. Selected Bond Angles (deg) for the $W_2Cl_2(NMe_2)_4(\mu\text{-}C_2H_2)(py)_2 \cdot CH_2Cl_2$ Molecule

A	B	C	angle	A	B	C	angle
W(2)	W(1)	Cl(3)	124.33 (5)	Cl(4)	W(2)	C(6)	162.74 (20)
W(2)	W(1)	N(7)	133.94 (18)	N(16)	W(2)	N(19)	85.36 (22)
W(2)	W(1)	N(10)	124.55 (15)	N(16)	W(2)	N(22)	171.28 (23)
W(2)	W(1)	N(16)	56.67 (16)	N(16)	W(2)	N(25)	87.32 (21)
W(2)	W(1)	N(19)	52.49 (15)	N(16)	W(2)	C(5)	74.96 (26)
W(2)	W(1)	C(5)	50.06 (19)	N(16)	W(2)	C(6)	96.31 (25)
W(2)	W(1)	C(6)	54.18 (22)	N(19)	W(2)	N(22)	103.19 (23)
Cl(3)	W(1)	N(7)	90.25 (18)	N(19)	W(2)	N(25)	168.38 (23)
Cl(3)	W(1)	N(10)	82.90 (16)	N(19)	W(2)	C(5)	104.28 (27)
Cl(3)	W(1)	N(16)	87.55 (17)	N(19)	W(2)	C(6)	75.22 (25)
Cl(3)	W(1)	N(19)	87.51 (15)	N(22)	W(2)	N(25)	83.96 (23)
Cl(3)	W(1)	C(5)	161.87 (21)	N(22)	W(2)	C(5)	104.13 (27)
Cl(3)	W(1)	C(6)	158.08 (21)	N(22)	W(2)	C(6)	87.67 (26)
N(7)	W(1)	N(10)	85.22 (23)	N(25)	W(2)	C(5)	82.44 (27)
N(7)	W(1)	N(16)	101.52 (24)	N(25)	W(2)	C(6)	114.62 (25)
N(7)	W(1)	N(19)	172.35 (23)	C(5)	W(2)	C(6)	37.9 (3)
N(7)	W(1)	C(5)	87.24 (26)	W(1)	N(7)	C(8)	121.0 (5)
N(7)	W(1)	C(6)	104.83 (27)	W(1)	N(7)	C(9)	130.2 (5)
N(10)	W(1)	N(16)	168.37 (22)	W(1)	N(10)	C(11)	125.1 (5)
N(10)	W(1)	N(19)	87.25 (21)	W(1)	N(10)	C(15)	118.1 (5)
N(10)	W(1)	C(5)	114.73 (25)	W(1)	N(16)	W(2)	71.13 (19)
N(10)	W(1)	C(6)	82.63 (26)	W(1)	N(16)	C(17)	116.6 (5)
N(16)	W(1)	N(19)	85.70 (22)	W(1)	N(16)	C(18)	122.6 (5)
N(16)	W(1)	C(5)	75.39 (26)	W(2)	N(16)	C(17)	116.3 (5)
N(16)	W(1)	C(6)	104.47 (27)	W(2)	N(16)	C(18)	123.2 (5)
N(19)	W(1)	C(5)	97.13 (25)	W(1)	N(19)	W(2)	71.08 (18)
N(19)	W(1)	C(6)	75.44 (25)	W(1)	N(19)	C(20)	124.0 (5)
C(5)	W(1)	C(6)	38.0 (3)	W(1)	N(19)	C(21)	117.1 (5)
W(1)	W(2)	Cl(4)	124.39 (5)	W(2)	N(19)	C(20)	121.8 (5)
W(1)	W(2)	N(16)	52.20 (15)	W(2)	N(19)	C(21)	116.6 (5)
W(1)	W(2)	N(19)	56.43 (16)	W(2)	N(22)	C(23)	129.6 (5)
W(1)	W(2)	N(22)	134.35 (17)	W(2)	N(22)	C(24)	123.6 (5)
W(1)	W(2)	N(25)	124.39 (15)	W(2)	N(25)	C(26)	123.5 (5)
W(1)	W(2)	C(5)	54.04 (21)	W(2)	N(25)	C(30)	119.7 (5)
W(1)	W(2)	C(6)	49.56 (20)	W(1)	C(5)	W(2)	75.90 (26)
Cl(4)	W(2)	N(16)	87.30 (16)	W(1)	C(5)	C(6)	65.8 (4)
Cl(4)	W(2)	N(19)	88.30 (17)	W(2)	C(5)	C(6)	75.6 (5)
Cl(4)	W(2)	N(22)	91.19 (18)	W(1)	C(6)	W(2)	76.26 (27)
Cl(4)	W(2)	N(25)	82.34 (17)	W(1)	C(6)	C(5)	76.2 (5)
Cl(4)	W(2)	C(5)	157.08 (22)	W(2)	C(6)	C(5)	66.5 (4)

Molecules of $W_2Cl_2(NMe_2)_4(\mu\text{-}C_2H_2)(py)_2$ (III) crystallize in the space group $P\bar{1}$, having virtual C_2 symmetry. Each tungsten atom in III achieves a pseudooctahedral coordination if the μ-C_2H_2 ligand is considered as one ligand site and the W–W bond is ignored. The two octahedral units are joined together in a confacial manner by a pair of NMe_2 ligands (N(16) and N(19)) and the μ-C_2H_2 ligand. The two tungsten atoms are joined by a metal–metal bond of length 2.597 (1) Å. Both this and the C–C distance of 1.38 (1) Å in the μ-C_2H_2 ligand are very similar to those observed in $W_2(O\text{-}i\text{-}Pr)_6(\mu\text{-}C_2H_2)(py)_2$.[4]

The NC_2 blades of the two terminal NMe_2 ligands N(7) and N(22)) are so aligned as to maximize π-donation from the lone pair of each nitrogen atom into the e set of orbitals (mostly a hybrid of metal based $d_{x^2-y^2}$ and d_{xy}) of each tungsten atom. The W–N bond distances, viz., ca. 1.985 (6) Å (average), reflect considerable double-bond order and are comparable to those found in 1,2-$W_2Cl_2(NMe_2)_4$ molecules.[5] This specific orientation of the terminal NMe_2 ligands has significant stereochemical consequences in the solid-state structure of $W_2Cl_2(NMe_2)_4(\mu\text{-}C_2H_2)(py)_2$ and apparently governs the overall chemistry of the other similar alkyne adducts. From a very close scrutiny of the ORTEP diagram presented in Figure 1, it becomes apparent that the μ-C_2H_2 ligand is distorted from an idealized perpendicular mode of bonding. The amount of deviation, θ (for an ideally perpendicular μ-alkyne, $\theta = 0$), is ca. 9°.

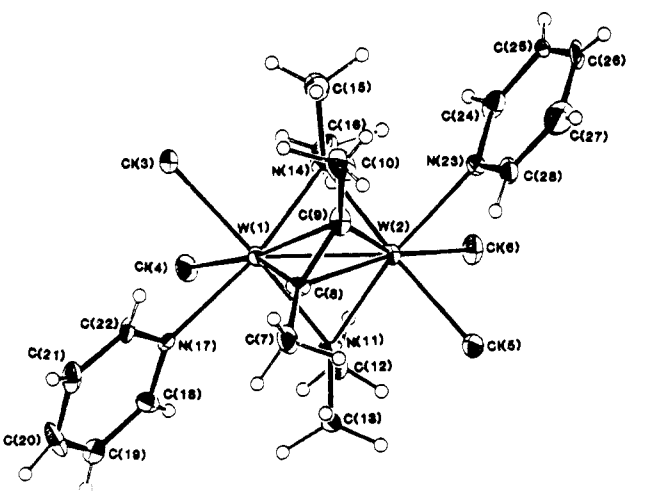

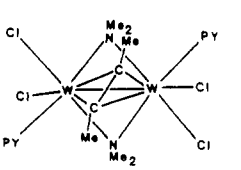

Figure 3. An ORTEP view of the $W_2Cl_4(NMe_2)_2(\mu\text{-}C_2Me_2)(py)_2$ molecule viewing down the virtual C_2 axis of symmetry, showing the skewed μ-C_2Me_2 moiety.

This deviation results in a small difference in the distances of the tungsten–carbon bonds between the μ-C_2H_2 ligand

(4) Chisholm, M. H.; Folting, K.; Hoffman, D. M.; Huffman, J. C. *J. Am. Chem. Soc.* **1984**, *106*, 6794.
(5) Akiyama, A.; Chisholm, M. H.; Cotton, F. A.; Extine, M. W., Murillo, C. A. *Inorg. Chem.* **1977**, *16*, 2407.

Table VI. Selected Bond Distances (Å) for the $W_2Cl_3(NMe_2)_3(\mu\text{-}PhC_2H)(py)_2 \cdot {}^1/_2C_7H_8$ Molecule

A	B	dist
W(1)	W(2)	2.6572 (16)
W(1)	Cl(3)	2.505 (3)
W(1)	Cl(4)	2.511 (4)
W(1)	N(17)	2.223 (11)
W(1)	N(23)	1.994 (11)
W(1)	N(32)	2.186 (10)
W(1)	C(6)	2.111 (13)
W(1)	C(7)	2.106 (12)
W(2)	Cl(4)	2.515 (4)
W(2)	Cl(5)	2.482 (3)
W(2)	N(14)	1.957 (11)
W(2)	N(26)	2.224 (10)
W(2)	N(32)	2.202 (10)
W(2)	C(6)	2.087 (12)
W(2)	C(7)	2.099 (13)
N(14)	C(15)	1.469 (19)
N(14)	C(16)	1.466 (17)
N(17)	C(18)	1.347 (17)
N(17)	C(22)	1.361 (18)
N(23)	C(24)	1.432 (19)
N(23)	C(25)	1.455 (18)
N(26)	C(27)	1.348 (17)
N(26)	C(31)	1.352 (17)
N(32)	C(33)	1.502 (17)
N(32)	C(34)	1.447 (17)
C(6)	C(7)	1.404 (18)
C(7)	C(8)	1.512 (19)
C–C(phenyl ring)[a]		1.390 (20)
C–C(pyridine)[a]		1.380 (20)

[a] Average.

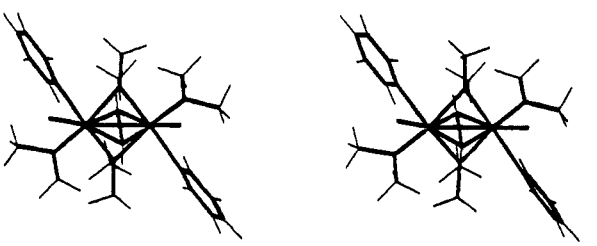

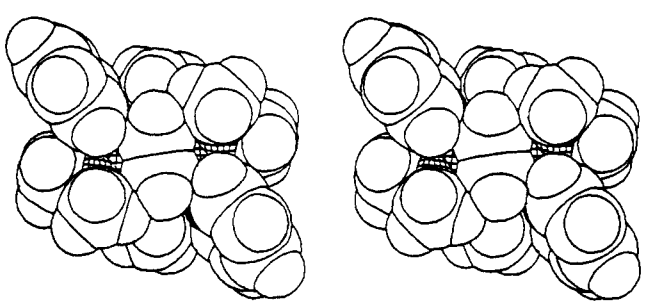

Figure 4. Space-filling diagrams of the $W_2Cl_2(NMe_2)_4(\mu\text{-}C_2H_2)(py)_2$ molecule, viewed down the virtual C_2 axis of symmetry and having the μ-C_2H_2 moiety on top.

and the tungsten atoms. Thus, the W(1)–C(6) and W(2)–C(5) distances are shorter by ca. 0.1 Å (average) than the W(1)–C(5) and W(2)–C(6) distances. This slight twist of the bridging ethyne ligand is presumably caused due to steric congestion imposed by the proximal methyl groups of the terminal NMe_2 ligands (C(23) and C(9)). This steric interaction can be seen in a computer-generated space-filling model shown in Figure 4, where C(5) and C(6) of the μ-C_2H_2 ligand are seen to have considerable inter-

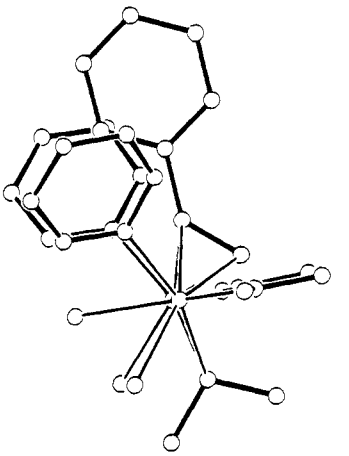

Figure 5. A ball and stick view of the $W_2Cl_3(NMe_2)_3(\mu\text{-}PhC_2H)(py)_2$ molecule looking down the W–W bond vector and perpendicular to the virtual mirror plane of symmetry. The view emphasizes the pseudooctahedral coordination of the W atoms when the μ-PhC_2H moiety is considered to occupy one ligand site. It also highlights the position of the phenyl ring such that one of the ortho protons is sandwiched between the pyridine rings, which greatly affects the ^1H NMR chemical shift of the former (see text).

action with the methyl groups of the NMe_2 ligand. The steric congestion would have been greater if the μ-C_2H_2 moiety were to orient in a perpendicular fashion. It is conceivable, at this point, that alkyl or aryl substituents on the μ-acetylene ligand would induce more steric congestion in the molecule and make it labile toward ligand redistribution reactions, as has been observed for $W_2Cl_2(NMe_2)_4(\mu\text{-}C_2Me_2)(py)_2$ and $W_2Cl_2(NMe_2)_4(\mu\text{-}PhC_2H)(py)_2$.

The NC_2 plane of each of the coordinated pyridine ligands is oriented in a way close to being perpendicular to the W–W bond axis. This presumably minimizes steric interactions and allows the NC_5H_5 ligands to coordinate fairly strongly to the tungsten atoms; W–N distances = ca. 2.260 (6) Å (average). Other distances and angles are close to what might have been expected.

Molecules of $W_2Cl_3(NMe_2)_3(\mu\text{-}PhC_2H)(py)_2$ (V) crystallize in the space group $P2_1/n$. Once again each tungsten atom is seen to attain a share of six ligands if the μ-PhC_2H ligand is considered one ligand site. Contrary to what has been seen in the structure of III, the two octahedral units in V are joined in a confacial manner through the agency of the μ-PhC_2H (perpendicular) ligand, the NMe_2 (N(32)) and the Cl(4) ligands, generating a virtual plane of symmetry containing these bridging ligands and bisecting the W–W bond axis (see Figure 5). The C–C distance of 1.40 (2) Å of the μ-PhC_2H ligand as well as the W–W distance of 2.657 (1) Å are comparable to those observed in $W_2(O\text{-}t\text{-}Bu)_6(py)(\mu\text{-}C_2H_2)$,[4] although the geometry of the latter compound is more akin to having two fused pseudo trigonal bipyramids in the solid state. The μ-PhC_2H ligand in compound V bridges the W–W bond in a perpendicular manner, and the four W-C distances (W(1)–C(6), W(1)–C(7), W(2)–C(6), and W(2)–C(7)) are almost identical, ca. 2.10 (1) Å (average). All other metal–ligand distances are similar to those in III and fall within 3σ.

It is interesting to point out here that the three NMe_2 ligands—the bridging, N(32), and the two terminal ones, N(14) and N(23)—are on the same side of the molecule. This particular arrangement arises presumably to minimize steric repulsions between the NMe_2 ligands and the phenyl ring of the μ-PhC_2H ligand. Also, orienting the terminal NMe_2 ligands trans to the μ-NMe_2 ligand would result in an unfavorable situation due to the mutual high trans

Table VII. Selected Bond Angles (deg) for the $W_2Cl_3(NMe_2)_3(\mu\text{-}PhC_2H)(py)_2 \cdot {}^1/_2C_7H_8$ Molecule

A	B	C	angle	A	B	C	angle
W(2)	W(1)	Cl(3)	126.67 (8)	Cl(5)	W(2)	C(6)	159.9 (4)
W(2)	W(1)	Cl(4)	58.16 (8)	Cl(5)	W(2)	C(7)	159.6 (4)
W(2)	W(1)	N(17)	124.55 (26)	N(14)	W(2)	N(26)	86.4 (4)
W(2)	W(1)	N(23)	131.5 (3)	N(14)	W(2)	N(32)	106.6 (4)
W(2)	W(1)	N(32)	53.01 (26)	N(14)	W(2)	C(6)	84.3 (5)
W(2)	W(1)	C(6)	50.3 (3)	N(14)	W(2)	C(7)	106.5 (5)
W(2)	W(1)	C(7)	50.7 (3)	N(26)	W(2)	N(32)	164.9 (4)
Cl(3)	W(1)	Cl(4)	83.24 (11)	N(26)	W(2)	C(6)	114.2 (4)
Cl(3)	W(1)	N(17)	82.95 (27)	N(26)	W(2)	C(7)	83.5 (4)
Cl(3)	W(1)	N(23)	88.8 (3)	N(32)	W(2)	C(6)	75.5 (4)
Cl(3)	W(1)	N(32)	88.0 (3)	N(32)	W(2)	C(7)	99.6 (4)
Cl(3)	W(1)	C(6)	159.7 (3)	C(6)	W(2)	C(7)	39.2 (5)
Cl(3)	W(1)	C(7)	159.8 (4)	W(1)	Cl(4)	W(2)	63.83 (9)
Cl(4)	W(1)	N(17)	86.2 (3)	W(2)	N(14)	C(15)	131.9 (9)
Cl(4)	W(1)	N(23)	170.3 (3)	W(2)	N(14)	C(16)	122.3 (9)
Cl(4)	W(1)	N(32)	80.24 (28)	C(15)	N(14)	C(16)	105.7 (10)
Cl(4)	W(1)	C(6)	104.8 (3)	W(1)	N(17)	C(18)	123.4 (9)
Cl(4)	W(1)	C(7)	79.9 (3)	W(1)	N(17)	C(22)	120.0 (10)
N(17)	W(1)	N(23)	87.3 (4)	C(18)	N(17)	C(22)	116.7 (12)
N(17)	W(1)	N(32)	164.5 (4)	W(1)	N(23)	C(24)	131.7 (9)
N(17)	W(1)	C(6)	115.8 (4)	W(1)	N(23)	C(25)	120.2 (9)
N(17)	W(1)	C(7)	85.0 (5)	C(24)	N(23)	C(25)	108.0 (11)
N(23)	W(1)	N(32)	105.1 (4)	W(2)	N(26)	C(27)	123.1 (8)
N(23)	W(1)	C(6)	84.5 (4)	W(2)	N(26)	C(31)	118.7 (9)
N(23)	W(1)	C(7)	106.7 (4)	C(27)	N(26)	C(31)	118.2 (12)
N(32)	W(1)	C(6)	75.3 (4)	W(1)	N(32)	W(2)	74.5 (3)
N(32)	W(1)	C(7)	99.9 (5)	W(1)	N(32)	C(33)	119.5 (8)
C(6)	W(1)	C(7)	38.9 (5)	W(1)	N(32)	C(34)	117.7 (8)
W(1)	W(2)	Cl(4)	58.01 (8)	W(2)	N(32)	C(33)	118.8 (8)
W(1)	W(2)	Cl(5)	126.83 (8)	W(2)	N(32)	C(34)	117.2 (8)
W(1)	W(2)	N(14)	132.4 (4)	C(33)	N(32)	C(34)	106.9 (11)
W(1)	W(2)	N(26)	123.57 (26)	W(1)	C(6)	W(2)	78.5 (4)
W(1)	W(2)	N(32)	52.46 (26)	W(1)	C(6)	C(7)	70.3 (7)
W(1)	W(2)	C(6)	51.1 (4)	W(2)	C(6)	C(7)	70.9 (7)
W(1)	W(2)	C(7)	50.9 (3)	W(1)	C(7)	W(2)	78.4 (4)
Cl(4)	W(2)	Cl(5)	83.31 (12)	W(1)	C(7)	C(6)	70.8 (8)
Cl(4)	W(2)	N(14)	169.6 (4)	W(1)	C(7)	C(8)	138.0 (9)
Cl(4)	W(2)	N(26)	86.2 (3)	W(2)	C(7)	C(6)	69.9 (8)
Cl(4)	W(2)	N(32)	79.9 (3)	W(2)	C(7)	C(8)	136.4 (9)
Cl(4)	W(2)	C(6)	105.5 (4)	C(6)	C(7)	C(8)	134.5 (11)
Cl(4)	W(2)	C(7)	79.9 (4)	C(7)	C(8)	C(9)	120.7 (12)
Cl(5)	W(2)	N(14)	88.6 (3)	C(7)	C(8)	C(13)	119.3 (12)
Cl(5)	W(2)	N(26)	83.92 (28)	C(9)	C(8)	C(13)	120.0 (12)
Cl(5)	W(2)	N(32)	88.70 (27)	C(8)	C(9)	C(10)	121.3 (13)

Table VIII. Selected Bond Distances for (Å) for the $W_2Cl_4(NMe_2)_2(\mu\text{-}C_2Me_2)(py)_2$ Molecule

A	B	dist
W(1)	W(2)	2.4360 (10)
W(1)	Cl(3)	2.395 (3)
W(1)	Cl(4)	2.411 (3)
W(1)	N(11)	2.186 (9)
W(1)	N(14)	2.142 (9)
W(1)	N(17)	2.281 (9)
W(1)	C(8)	2.020 (11)
W(1)	C(9)	2.447 (11)
W(2)	Cl(5)	2.398 (3)
W(2)	Cl(6)	2.416 (3)
W(2)	N(11)	2.163 (9)
W(2)	N(14)	2.182 (9)
W(2)	N(23)	2.281 (10)
W(2)	C(8)	2.438 (11)
W(2)	C(9)	2.024 (11)
N(11)	C(12)	1.490 (19)
N(11)	C(13)	1.500 (17)
N(14)	C(15)	1.488 (15)
N(14)	C(16)	1.470 (16)
N(17)	C(18)	1.339 (16)
N(17)	C(22)	1.324 (16)
N(23)	C(24)	1.345 (16)
N(23)	C(28)	1.355 (16)
C(7)	C(8)	1.507 (19)
C(8)	C(9)	1.372 (17)
C(9)	C(10)	1.494 (18)
C–C(pyridine ring)[a]		1.367 (20)

[a] Average.

influence[6] of the NMe_2 groups.

$W_2Cl_4(NMe_2)_2(\mu\text{-}C_2Me_2)(py)_2$ (VI) crystallizes in the space group $P2_1/n$. As in the previously discussed alkyne adducts of d^3–d^3 W_2-containing compounds the geometry may superficially be viewed as derived from a confacial bioctahedron with the two bridging NMe_2 ligands and the centroid of the μ-C_2Me_2 moiety forming the common face (see Figure 6). The two octahedra are joined together by a W–W bond of distance 2.436 (1) Å. However, the μ-C_2Me_2 ligand in VI is severly distorted from the perpendicular alkyne bonding mode, and this is much more pronounced than the small distortion observed in III for which steric factors were thought to be responsible. A twist of 35° from the perpendicular orientation is measured. The torsion angle C–C–C–C of the μ-C_2Me_2 ligand is 42°. The C–C–C angle of 125° (averaged) is close to those normally seen in parallel alkyne adducts[7] (θ = 90°) and smaller than those typically seen for perpendicular alkyne adducts which span a range, 135–150°.[7] Similar distortions, but of lesser magnitude, have previously been seen for $Cp_2Nb_2(CO)_2(\mu\text{-}C_2Ph_2)_2$[8] and $W_2(O\text{-}t\text{-}Bu)_4(\mu\text{-}C_2Ph_2)_2$,[9]

(6) Appleton, T. G.; Clark, H. C.; Manzer, L. E. *Coord. Chem. Rev.* **1973**, *10*, 335.
(7) Hoffman, D. M.; Hoffmann, R.; Fisel, C. R. *J. Am. Chem. Soc.* **1982**, *104*, 3858.
(8) Nesmayanov, A. N.; Gusev, A. I.; Pasynskii, A. A.; Asisimov, K. N.; Kolobova, N. E.; Struchkov, Y. T. *J. Chem. Soc., Chem. Commun.* **1968**, 1365.

Table IX. Selected Bond Angles (deg) for the $W_2Cl_4(NMe_2)_2(\mu\text{-}C_2Me_2)(py)_2$ Molecule

A	B	C	angle	A	B	C	angle
W(2)	W(1)	Cl(3)	128.15 (8)	Cl(6)	W(2)	N(11)	92.0 (3)
W(2)	W(1)	Cl(4)	123.85 (8)	Cl(6)	W(2)	N(14)	88.22 (25)
W(2)	W(1)	N(11)	55.48 (25)	Cl(6)	W(2)	N(23)	79.43 (27)
W(2)	W(1)	N(14)	56.49 (24)	Cl(6)	W(2)	C(8)	167.2 (3)
W(2)	W(1)	N(17)	133.52 (24)	Cl(6)	W(2)	C(9)	158.2 (3)
W(2)	W(1)	C(8)	65.6 (3)	N(11)	W(2)	N(14)	94.4 (4)
W(2)	W(1)	C(9)	48.97 (27)	N(11)	W(2)	N(23)	169.3 (3)
Cl(3)	W(1)	Cl(4)	90.08 (11)	N(11)	W(2)	C(8)	75.3 (4)
Cl(3)	W(1)	N(11)	176.24 (26)	N(11)	W(2)	C(9)	108.5 (4)
Cl(3)	W(1)	N(14)	88.46 (26)	N(14)	W(2)	N(23)	91.6 (3)
Cl(3)	W(1)	N(17)	86.09 (26)	N(14)	W(2)	C(8)	93.2 (4)
Cl(3)	W(1)	C(8)	96.6 (3)	N(14)	W(2)	C(9)	83.0 (4)
Cl(3)	W(1)	C(9)	88.33 (27)	N(23)	W(2)	C(8)	113.2 (4)
Cl(4)	W(1)	N(11)	88.09 (27)	N(23)	W(2)	C(9)	80.9 (4)
Cl(4)	W(1)	N(14)	91.53 (26)	C(8)	W(2)	C(9)	34.2 (4)
Cl(4)	W(1)	N(17)	79.35 (26)	W(1)	N(11)	W(2)	68.14 (27)
Cl(4)	W(1)	C(8)	159.7 (3)	W(1)	N(11)	C(12)	122.4 (9)
Cl(4)	W(1)	C(9)	166.0 (3)	W(1)	N(11)	C(13)	121.5 (8)
N(11)	W(1)	N(14)	94.9 (4)	W(2)	N(11)	C(12)	118.8 (9)
N(11)	W(1)	N(17)	90.3 (4)	W(2)	N(11)	C(13)	118.2 (8)
N(11)	W(1)	C(8)	84.0 (4)	W(1)	N(14)	W(2)	68.57 (26)
N(11)	W(1)	C(9)	94.2 (4)	W(1)	N(14)	C(15)	120.7 (8)
N(14)	W(1)	N(17)	169.4 (3)	W(1)	N(14)	C(16)	119.2 (8)
N(14)	W(1)	C(8)	107.8 (4)	W(2)	N(14)	C(15)	120.9 (8)
N(14)	W(1)	C(9)	74.5 (4)	W(2)	N(14)	C(16)	120.8 (8)
N(17)	W(1)	C(8)	82.0 (4)	W(1)	N(17)	C(18)	121.6 (8)
N(17)	W(1)	C(9)	114.4 (4)	W(1)	N(17)	C(22)	120.6 (8)
C(8)	W(1)	C(9)	34.1 (4)	W(2)	N(23)	C(24)	123.9 (9)
W(1)	W(2)	Cl(5)	128.09 (8)	W(2)	N(23)	C(28)	119.3 (8)
W(1)	W(2)	Cl(6)	123.94 (8)	W(1)	C(8)	W(2)	65.5 (3)
W(1)	W(2)	N(11)	56.39 (26)	W(1)	C(8)	C(7)	144.2 (10)
W(1)	W(2)	N(14)	54.94 (24)	W(1)	C(8)	C(9)	90.3 (8)
W(1)	W(2)	N(23)	133.92 (22)	W(2)	C(8)	C(7)	138.1 (9)
W(1)	W(2)	C(8)	48.97 (27)	W(2)	C(8)	C(9)	56.1 (6)
W(1)	W(2)	C(9)	65.8 (3)	C(7)	C(8)	C(9)	124.7 (12)
Cl(5)	W(2)	Cl(6)	90.37 (11)	W(1)	C(9)	W(2)	65.2 (3)
Cl(5)	W(2)	N(11)	88.52 (26)	W(1)	C(9)	C(8)	55.6 (6)
Cl(5)	W(2)	N(14)	176.79 (25)	W(1)	C(9)	C(10)	139.3 (9)
Cl(5)	W(2)	N(23)	85.26 (24)	W(2)	C(9)	C(8)	89.7 (7)
Cl(5)	W(2)	C(8)	88.8 (3)	W(2)	C(9)	C(10)	143.6 (9)
Cl(5)	W(2)	C(9)	97.3 (3)	C(8)	C(9)	C(10)	125.6 (11)

complexes having two bridging alkyne ligands which have angles of twist θ = 11 and 20°, respectively.

Initially one might wish to attribute the twisting of the μ-C–C bond vector to steric pressure imposed by the ligands, especially the μ-NMe_2 ligands which have proximal and distal methyl groups with respect to the μ-C_2Me_2 functionality. However, there is no apparent distortion of the μ-NMe_2 ligands, and the bond distances and angles are very similar to those in III and V. Moreover, space-filling diagrams, shown in Figure 7, do not support the notion that twisting occurs to relieve steric repulsive interactions. The feature in VI which has not been encountered previously is the presence of four Cl ligands in lieu of strong π-donor ligands, such as NMe_2 or OR, in the terminal positions. This could bring about changes in the electronic nature of the molecule that may result in a twist of the μ-C_2Me_2 ligand.

Bonding Considerations. As in $W_2(OR)_6(\mu\text{-}C_2R_2)(py)_n$[1] compounds (R = *t*-Bu, *n* = 1, R′ = H; *R* = *i*-Pr, *n* = 2, R′ = H; R = CH_2-*t*-Bu, *n* = 2, R′ = H; R = CH_2-*t*-Bu, *n* = 1, R′ = Me, Et, and Ph), the bridging ligands in III and V are considered as μ-$C_2R_2^{4-}$ moieties spanning a $(W\text{-}W)^{10+}$ center. The relatively long W–W and C–C distances suggest that this would be an appropriate view. In this description, extensive W-to-C_2R_2 π^* bonding results in limiting W–W and C–C single bonds and formation of a dimetallatetrahedrane, I. $W_2Cl_4(NMe_2)_2(\mu\text{-}C_2Me_2)(py)_2$,

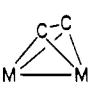

I

on the other hand, shows significant deviation from such a description. Instead, it shows incipient 1,2-dimetallacyclobutadiene characteristics. The W—W distance of 2.436 (1) Å is typical of a $(W{=}W)^{8+}$ bonding distance[10] and is notably shorter than those in perpendicular alkyne adducts of the $(W\text{-}W)^{10+}$ center, which fall in the range 2.55–2.67 Å. The two very different W–C distances, 2.02 and 2.44 Å, are approaching M–C double[4,11] and nonbonding distances, respectively. Note that the W–C distance of 2.02 Å is shorter than those seen in the ditungstatetrahedranes, ca. 2.10 Å. The ^{13}C chemical shift (discussed in the next section) of the μ-C_2 carbon atoms is also notably different.

This leads to the suggestion that the $W_2(\mu\text{-}C_2Me_2)$ moiety has bonding contributions that may be depicted by the valence bond descriptions shown in IIa and IIb. These are intermediates between the limiting dimetallatetrahedrane and planar 1,2-dimetallacyclo-

(9) Cotton, F. A.; Schwotzer, W.; Shamshoum, E. S. *Organometallics* **1983**, *2*, 1167.

(10) For a listing of W–W bond distances and W–W bond order assignments, see: Chisholm, M. H. *Polyhedron* **1983**, *2*, 681.

(11) Chisholm, M. H.; Hoffman, D. M.; Huffman, J. C. *J. Am. Chem. Soc.* **1984**, *106*, 6815.

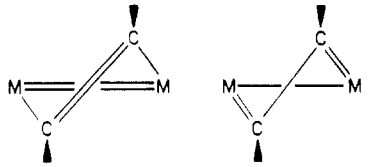

IIa IIb

butadiene descriptions that may be formed by the coupling of M≡M and C≡C bonds in the perpendicular and parallel modes, respectively.

NMR Spectroscopic Studies. The ^1H and ^{13}C NMR spectra of the alkyne adducts are reported in the Experimental Section, and some salient features are discussed below. The ^1H NMR spectrum of $W_2Cl_2(NMe_2)_4(\mu\text{-}C_2H_2)(py)_2$ is consistent with that expected based upon the structure shown in Figure 1. Both halves of the molecule are equivalent due to the presence of a C_2 axis of symmetry, giving rise to four singlets of equal intensity for the methyl groups of the NMe_2 ligands. Rotations around the W–N bonds of the terminal NMe_2 ligands are very slow at ambient temperatures as suggested by the appearance of separate proximal and distal methyl resonances, which is consistent with the observed short W–N bond distances in the solid-state structure.[3] It should be noted here that the resonances for the proximal and distal methyl groups are not widely separated, contrary to what is observed for NMe_2 groups bonded to $(W{\equiv}W)^{6+}$ centers.[12] This is again consistent with the absence of a metal–metal triple bond in $W_2Cl_2(NMe_2)_4(\mu\text{-}C_2H_2)(py)_2$. The coordinated pyridine ligands are not labile on the NMR time scale and exhibit two different resonances for the protons in each of the ortho and meta positions, indicating restricted rotations around the W–NC_5H_5 bonds. This presumably arises due to steric congestion in the molecule.

The ^1H resonance of the μ-C_2H_2 ligand, ca. 7.35 ppm, is shifted considerably downfield relative to that in free acetylene, ca. 1.80 ppm.[13] The former chemical shift value is comparable to those in $W_2(OR)_6(\mu\text{-}C_2H_2)(py)_n$[1] compounds. However, whereas no $^2J_{^{183}W\text{-}^1H}$ has been observed in the latter compound, a coupling constant $^2J_{^{183}W\text{-}^1H}$ of ca. 5.3 Hz has been observed for the μ-C_2H_2 ligand in $W_2Cl_2(NMe_2)_4(\mu\text{-}C_2H_2)(py)_2$.

The ^{13}C NMR spectrum of the labeled (92.5 g atom % ^{13}C) $W_2Cl_2(NMe_2)_4(\mu\text{-}{*}C_2H_2)(py)_2$ is also very informative. The spectrum of the μ-$*C_2H_2$ ligand in the complex is shown in Figure 8. In the ^1H decoupled spectrum (Figure 8a), the coordinated ethyne carbons appear as a singlet, as expected, at δ 162.2 relative to Me_4Si and show coupling to ^{183}W ($I = {}^1/_2$, 14.3% natural abundance). The satellite signals with ca. 13.4% intensity (labeled x) relative to the main peak are due to the isotopomer having one ^{183}W nucleus, and the signals of intensity ca. 2% (labeled y) are due to the isotopomer having two ^{183}W nuclei. The observed $^1J_{^{183}W\text{-}^{13}C}$, ca. 36 Hz, is comparable to that found for $W_2(O\text{-}i\text{-}Pr)_6(\mu\text{-}{*}C_2H_2)(py)_2$. Also notable here is the appearance of only one kind of $^1J_{^{183}W\text{-}^{13}C}$ value, although a small difference, ca. 0.10 Å, is observed in the W–C bond distances in the solid state. The ^1H-coupled spectrum, shown in Figure 8b, exhibits an AA′XX′ spin pattern, neglecting the signals arising due to ^{183}W–^{13}C coupling (denoted by an asterisk). The various coupling constants that have been extracted from an analysis[14] of this spectrum are $^1J_{^{13}C\text{-}H} = 190$ Hz, $^2J_{^{13}C\text{-}H} = 2.0$ Hz, $^1J_{^{13}C\text{-}^{13}C} = 18.5$ Hz, and $^3J_{H\text{-}H} = 1.6$ Hz. The relative signs of $^1J_{C\text{-}H}$ and $^2J_{C\text{-}H}$ are the same, and with the assumption that $^1J_{C\text{-}H}$ is positive,[15] the sign of $^2J_{C\text{-}H}$ would be positive also. The relative signs of $^1J_{C\text{-}C}$ and $^3J_{H\text{-}H}$ remain undetermined. The observed $^1J_{C\text{-}H}$ value is intermediate to those for $H_2C{=}CH_2$ and HC≡CH, 156 and 249 Hz, respectively. Strained ring systems, e.g., cyclopropane and bicyclobutane, have comparable $^1J_{C\text{-}H}$ values.[16,17] The absolute value of the observed $^2J_{CH}$ is comparable to that found in ethylene (−2.4 Hz) and cyclopropane (−2.6 Hz). Most interestingly, the ^{13}C–^{13}C coupling constant of 18.5 Hz is very small compared to the J_{CC} = 35, 68, and 172 Hz for ethane,

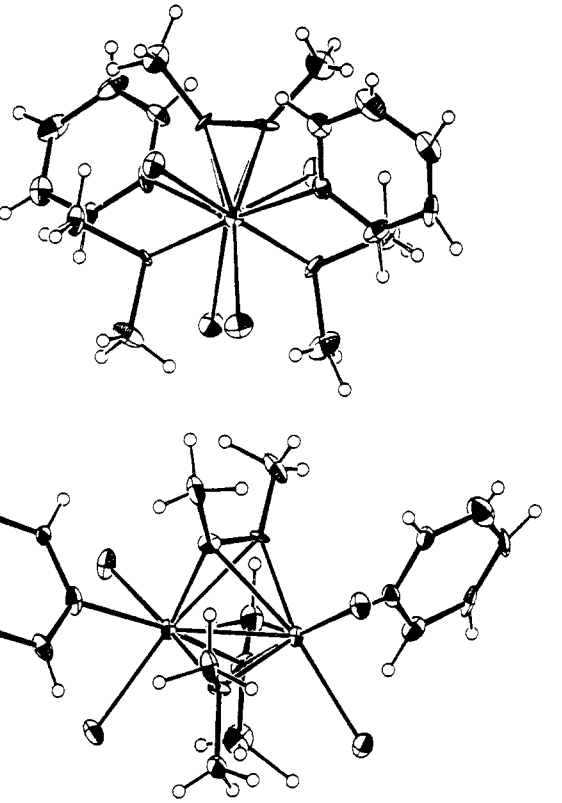

Figure 6. Views of the $W_2Cl_4(NMe_2)_2(\mu\text{-}C_2Me_2)(py)_2$ molecule looking down the W–W axis (top) and looking perpendicular to the W–W bond (bottom).

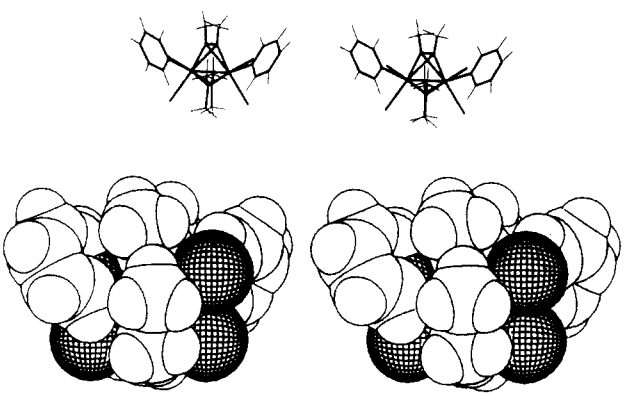

Figure 7. Space-filling diagrams of the $W_2Cl_4(NMe_2)_2(\mu\text{-}C_2Me_2)(py)_2$ molecule.

(12) Chisholm, M. H.; Haitko, D. A.; Folting, K.; Huffman, J. C. *J. Am. Chem. Soc.* **1981**, *103*, 4046.
(13) Silverstein, R. M.; Bassler, G. C.; Morrill, T. C. In *Spectrometric Identification of Organic Compounds*, 4th ed.; Wiley: New York, 1981.
(14) Gunther, H. *Angew. Chem., Int. Ed. Engl.* **1972**, *11*, 861.
(15) (a) Buckingham, A. D.; McLauchlan, K. A. *Proc. Chem. Soc.* **1963**, 144. (b) Bernheim, R. A.; Lavery, B. J. *J. Am. Chem. Soc.*, **1967**, *89*, 1279. (c) Spiesecke, H. *Z. Naturforsch., A: Astrophys., Phys. Phys. Chem.* **1968**, *23A*, 467.
(16) Marshall, J. L. *Methods Stereochem. Anal.* **1983**, *2*, 11.
(17) Stothers, J. B. *Carbon-13 NMR Spectroscopy*; Academic Press: New York, 1972.

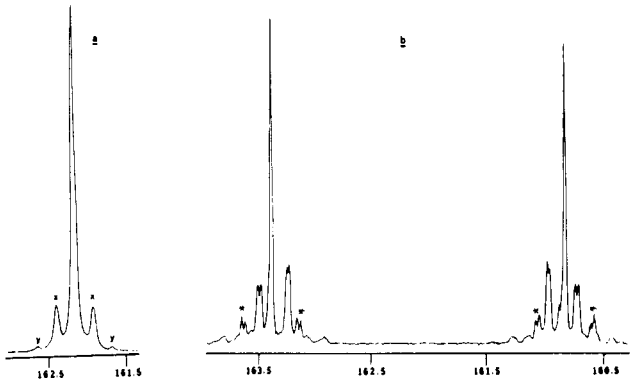

Figure 8. ^{13}C NMR spectra of $W_2Cl_2(NMe_2)_4(\mu\text{-}{*}C_2H_2)(py)_2$ (where *C represents 92.5 g atom % ^{13}C) in CD_2Cl_2, at 23 °C and at 75 MHz, in the scale expanded regions showing the resonances due to the μ-$*C_2H_2$ ligand. (a) ^1H-decoupled spectrum showing coupling to ^{183}W ($I = {}^1/_2$, 14.3% natural abundance) (denoted by x); satellite signals denoted by y are due to the isotopomer having two ^{183}W nuclei. (b) ^1H-coupled spectrum exhibiting an AA'XX' spin pattern; satellite signals due to ^{183}W are denoted by an asterisk.

ethylene, and ethyne, respectively, and is best compared to the values observed in three-membered-ring systems.[16,17] This seems to be a common feature in ditungstatetrahedra, $W_2(\mu\text{-}C_2H_2)$-containing compounds,[1] and parallels the small $^1J_{CC}$ value recently reported for $C_4(t\text{-}Bu)_4$.[18]

The ^1H NMR spectrum of $W_2Cl_2(NMe_2)_4(\mu\text{-}C_2Me_2)(py)_2$, which has to be recorded at low temperatures to suppress the facile ligand redistribution reaction, is fully consistent with the adoption of a structure analogous to the ethyne adduct. $W_2Cl_2(NMe_2)_4(\mu\text{-}MeC_2H)(py)_2$, on the other hand, adopts a different geometry as determined by ^1H NMR spectroscopy. The spectrum is consistent with having a mirror plane of symmetry in the molecule giving rise to four different resonances for the methyl groups of the μ-NMe_2 ligands and two resonances of twice the intensity for the proximal and distal methyl groups of the two equivalent terminal NMe_2 ligands. The adduct of the unsymmetrical alkyne PhC≡CH also exhibits a very similar ^1H NMR spectrum and is believed to have a similar structure. $W_2Cl_3(NMe_2)_3(\mu\text{-}PhC_2H)(py)_2{\cdot}{}^1/_2C_7H_8$ also contains a mirror plane of symmetry, and the ^1H NMR spectrum of the complex is fully consistent with the expectations based on the solid-state structure. The phenyl ring of the μ-PhC_2H moiety shows very slow rotation on the NMR time scale at ambient temperatures. It is interesting to note here that the observed orientation of the phenyl ring (being nearly coplanar with the mirror plane of symmetry as well as the pyridine rings) as seen in the solid-state structure is preserved in solutions (see Figure 5). As a result, the "ring current" effect of the pyridine ligands shifts one of the ortho protons upfield to ca. 4.54 ppm.

^1H NMR spectra of $W_2Cl_4(NMe_2)_2(\mu\text{-}C_2Me_2)(py)_2$ show two singlets for the methyl groups of the μ-NMe_2 ligands at room temperatures, indicative of retaining the solid-state structure in solution. The spectrum also suggests rapid rotation, on the NMR time scale, of the pyridine ligands around the W–N bonds. The ^{13}C chemical shift value of the μ-CMe_2 ligand, ca. 214 ppm relative to Me_4Si, is suggestive of alkylidene character[4] and notably downfield from the range of carbon chemical shifts (120–160 ppm) observed in other perpendicularly bridged $W_2(\mu\text{-}C_2R_2)$-containing compounds.

(18) Loerzer, T.; Machinek, R.; Luttke, W.; Franz, L. H.; Malsch, K. D.; Maier, G. *Angew. Chem., Int. Ed. Engl.*, **1983**, *22*, 878.

Concluding Remarks

So far, reactions of $W_2Cl_2(NMe_2)_4$ with alkynes, in the presence of pyridine, have failed to yield any products resulting from the cleavage of W≡W and C≡C bonds. (Reactions in the absence of pyridine produce as yet uncharacterizable products.) This is probably due to the less steric demand of the NMe_2 ligands compared to the alkoxide ligands. Nonetheless, interesting and unusual $W_2(\mu\text{-}C_2R_2)$-containing compounds were formed in these reactions. Especially, the discovery of $W_2Cl_4(NMe_2)_2(\mu\text{-}C_2Me_2)(py)_2$, formed as a result of a ligand redistribution reaction of $W_2Cl_2(NMe_2)_4(\mu\text{-}C_2Me_2)(py)_2$, provides the first example of an intermediate geometry for the interconversion of a perpendicular alkyne (a dimetallatetrahedrane) with a parallel alkyne complex[19] (a 1,2-dimetallacyclobutadiene). Though deviations from the idealized perpendicular and parallel modes of bonding have previously been observed, the twisting has always been relatively small.[8,9] This finding contrasts with over a dozen structurally characterized alkyne adducts of d^3–d^3 tungsten dimers,[1] all of which adopt the perpendicular bonding mode. In view of the present finding it is interesting to speculate that the conversion of a perpendicular to a parallel bonding mode for the alkyne may be involved in the reaction pathway leading to metathesis of W≡W and C≡C bonds.[20,21] An explanation for the observed twisting of the μ-C_2Me_2 ligand in VI is presented by Hoffmann and co-workers in a following paper.

Experimental Section

All operations were carried out in dry and oxygen-free atmosphere (N_2). Properly dried and deoxygenated solvents were used throughout. $W_2Cl_2(NMe_2)_4$ was prepared according to literature methods.[5] Nicolet 360-MHz and Varian XL300 NMR instruments were used to obtain ^1H and ^{13}C NMR spectra, respectively. Infrared spectra were obtained from a Perkin-Elmer 283 instrument using Nujol mulls.

$W_2Cl_2(NMe_2)_4(\mu\text{-}C_2H_2)(py)_2{\cdot}CH_2Cl_2$. A suspension of $W_2Cl_2(NMe_2)_4$ (0.26 g, 0.41 mmol) was made in toluene (4 mL), pyridine (0.1 mL) was added, and the whole mixture was cooled to −196 °C. HC≡CH (1 equiv) was transferred on to the frozen reaction mixture via a calibrated vacuum manifold and rapidly warmed to 0 °C. The reaction mixture was stirred at that temperature for ${}^1/_2$ h, then brought to room temperature, and stirred for another 45 min. A red-brown microcrystalline precipitate was formed, collected by filtration, and dried under vacuum. The solid was redissolved in CH_2Cl_2 (5 mL), and dark red needles of $W_2Cl_2(NMe_2)_4(\mu\text{-}C_2H_2)(py)_2{\cdot}CH_2Cl_2$ were obtained by slow diffusion of hexane; yield 0.22 g (62%). Anal. Calcd for $W_2Cl_4N_6C_{21}H_{38}$: C, 28.5; H, 4.3; N, 9.5; Cl, 16.0. Found: C, 28.4; H, 4.5; N, 9.6; Cl, 16.1.

IR data (Nujol, NaCl plates): 3200 (m), 2805 (m), 2760 (m), 1598 (m), 1480 (m), 1441 (s), 1262 (m), 1209 (m), 950 (s), 920 (m, br), 760 (s), 700 (s) cm^{-1}.

^1H NMR spectral data (from CD_2Cl_2 at 21 °C, δ values reported relative to Me_4Si): δ 2.66 (s, 6 H, NMe_2), 2.85 (s, 6 H, NMe_2), 3.06 (s, 6 H, NMe_2), 3.30 (s, 6 H, NMe_2), 7.32 (br, 2 H, NC_5H_5), 7.35 (s, 2 H, μ-C_2H_2), 7.55 (br, 2 H, NC_5H_5), 7.85 (m, 2 H, NC_5H_5), 8.51 (br, 2 H, NC_5H_5), 9.39 (br, 2 H, NC_5H_5).

^{13}C NMR data of the μ-$*C_2H_2$ (*C represents 92.5 gm atom % ^{13}C) ligand (from CD_2Cl_2 at 21 °C): δ 162.2 (J_{WC} = 36 Hz, $^1J_{CH}$ = 190 Hz, $^2J_{CH}$ = 2.0 Hz, J_{CC} = 18.5 Hz).

$W_2Cl_2(NMe_2)_4(\mu\text{-}C_2Me_2)(py)_2{\cdot}py$. Similar mixing procedures, as in the previous case, were followed. The reaction mixture was

(19) Generally, structural types having either parallel or perpendicularly bridged alkynes are seen. Hoffman et al.[7] have elaborated upon the reasons for this general occurrence and noted that the preference for one structure over the other has in most instances an understandable electronic origin.

(20) Schrock, R. R.; Listemann, M. L.; Sturgeoff, L. G. *J. Am. Chem. Soc.* **1982**, *104*, 4291.

(21) Listemann, M. L.; Schrock, R. R. *Organometallics* **1985**, *4*, 74.

Table X. Summary of Crystallographic Data[a]

	III	V	VI
Fw	884.08	912.69	809.96
space group	$P\bar{1}$	$P2_1/n$	$P2_1/n$
a, Å	17.123 (5)	14.701 (7)	10.918 (4)
b, Å	12.012 (3)	12.137 (6)	13.440 (5)
c, Å	7.410 (1)	17.632 (9)	16.558 (7)
α, deg	105.80 (1)	103.15 (3)	104.45 (2)
β, deg	94.71 (1)		
γ, deg	101.93 (1)		
Z	2	4	4
V, Å^3	1419.33	3063.60	2352.77
d_{calcd}, g cm^{-3}	2.069	1.979	2.287
cryst size, mm	0.12 × 0.12 × 0.10	0.12 × 0.24 × 0.16	0.07 × 0.06 × 0.06
cryst color	black	black	yellow-green
radiatn	Mo Kα (λ = 0.71069 Å) graphite monochromator		
linear absorptn coeff, cm^{-1}	86.758	79.560	104.548
transmissn factors	no abs corr	no abs corr	0.2320–0.3600
temp, °C	−160	−161	−160
instrument	Picker four-circle diffractometer locally modified and interfaced		
detector aperture	3.0 × 4.0	3.0 × 4.0	3.0 × 4.0
sample to source dist, cm^{-1}	23.5	23.5	23.5
takeoff angle, deg	2.0	2.0	2.0
scan speed, deg/min	4.0	6.0	4.0
scan width, deg	2.0 + 0.692 tan θ	1.5 + 0.692 tan θ	2.0 + 0.692 tan θ
bkgd counter, s, at each end of scan	8	6	8
2θ range, deg	6–45	6–45	6–45
data collected	3960	5449	4173
unique data	3707	4016	3093
unique data with $F_o > 2.33\sigma(F_o)$	3358	3254	2671
$R(F)$	0.0263	0.0450	0.0390
$R_w(F)$	0.0287	0.0450	0.0405
goodness of fit	0.907	0.971	1.403
largest Δ/σ	0.05	0.05	0.05

[a] III, $W_2Cl_2(NMe_2)_4(\mu\text{-}C_2H_2)(py)_2\cdot CH_2Cl_2$; V, $W_2Cl_3(NMe_2)_3(\mu\text{-}PhC_2H)(py)_2\cdot{}^1/_2C_7H_8$; VI, $W_2Cl_4(NMe_2)_2(\mu\text{-}C_2Me_2)(py)_2$.

quickly brought to room temperature and stirred for $2^1/_2$ h by which time dark blue-green microcrystals were formed. The solid was separated by filtration, washed with toluene (5 mL), and dried under vacuum; yield of $W_2Cl_2(NMe_2)_4(C_2Me_2)(py)_2\cdot py$: 71%. Due to thermal instability of the compound significant amounts of impurity were always present, which is reflected in the poor elemental analysis and the presence of uncalled for resonances in the NMR spectra. Anal. Calcd for $W_2Cl_2N_7C_{27}H_{45}$: C, 32.3; H, 4.5; N, 9.8; Cl, 7.1. Found: C, 31.8; H, 4.4; N, 8.9; Cl, 8.1.

IR data (Nujol, NaCl plates): 3190 (m), 2762 (m), 2600 (m), 1600 (m), 1490 (m), 1440 (s), 1209 (m), 952 (s), 758 (s), 695 (s) cm^{-1}.

^{1}H NMR data (−45 °C, CD_2Cl_2, δ relative to Me_4Si): δ 7.10–9.25 (m, 15 H, NC_5H_5), 3.10 (s, 6 H, NMe_2), 2.96 (s, 6 H, NMe_2), 2.84 (s, 6 H, NMe_2), 2.80 (s, 6 H, NMe_2), 2.38 (s, 6 H, C_2Me_2).

$W_2Cl_2(NMe_2)_4(\mu$-$MeC_2H)(py)_2$. A suspension of $W_2Cl_2(NMe_2)_4$ (0.40 g, 0.65 mmol) was made in toluene (4 mL), and pyridine (ca. 3.5 equiv) was added. The mixture was cooled to −196 °C, and MeC≡CH (1 equiv) was transferred onto this frozen mixture by using a calibrated vacuum manifold. It was warmed to room temperature and stirred for 15 min, by which time the reaction was complete. The color changed from yellow to dark green. The volatile components of the reaction mixture were removed under vacuum, and the solid residue was redissolved in toluene (3 mL) and layered with hexane on top. Microcrystalline $W_2Cl_2(NMe_2)_4(\mu\text{-}MeC_2H)(py)_2$ precipitated; yield 0.18 g (35%). Due to the thermal instability of this compound, the prepared samples could never be made completely devoid of impurities. Anal. Calcd for $W_2Cl_2N_6C_{21}H_{38}$: C, 30.4; H, 4.6; N, 10.1; Cl, 8.6. Found: C, 30.1; H, 4.4; N, 9.7; Cl, 8.9.

IR data (Nujol, NaCl plates): 2800 (m), 1600 (m), 1480 (m), 1440 (s), 1410 (m), 1360 (m), 1258 (m), 1015 (m), 940 (s), 995 (m, br), 755 (m), 700 (m) cm^{-1}.

^{1}H NMR data (toluene-d_8, 21 °C, δ relative to Me_4Si): δ 2.12 (s, 3 H, $HC_2\mathit{Me}$), 2.80 (br s, 3 H, NMe_2), 3.06 (br s, 3 H, NMe_2), 3.17 (s, 6 H, NMe_2), 3.23 (s, 6 H, NMe_2), 3.26 (br s, 3 H, NMe_2), 3.31 (br s, 3 H, NMe_2), 7.62 (s, 1 H, $\mathit{H}C_2Me$), 6.50–7.60 (m, 10 H, NC_5H_5).

$W_2Cl_3(NMe_2)_3(\mu$-$PhC_2H)(py)_2\cdot{}^1/_2C_7H_8$. PhC≡CH (65 μL) was added slowly, via a microliter syringe and at 0 °C, to a stirred suspension of $W_2Cl_2(NMe_2)_4$ (0.35 g, 0.6 mmol) in toluene (4 mL) and pyridine (0.25 mL). The color changed immediately, and dark green microcrystalline $W_2Cl_2(NMe_2)_4(\mu\text{-}PhC_2H)(py)_2$ started to precipitate out in 5 min. [The latter complex can be isolated in ca. 90% yield by filtration after ca. $^1/_2$-h reaction time.] The reaction mixture was stirred at ca. 60 °C for 6 h after which the color turned from dark green to brown. The solution was then left to cool to room temperature. Dark brown crystals of $W_2Cl_3(NMe_2)_3(\mu\text{-}PhC_2H)(py)_2\cdot{}^1/_2C_7H_8$ were collected after 2 days by filtration; yield 0.24 g (65%) according to eq 5. Anal. Calcd for $W_2Cl_3N_5C_{27.5}H_{38}$: C, 36.2; H, 4.2; N, 7.7; Cl, 11.7. Found: C, 36.4; H, 4.0; N, 7.9; Cl, 11.5.

IR data (Nujol, NaCl plates): 1600 (m), 1585 (m), 1490 (m), 1440 (s), 1410 (m), 1210 (m), 1065 (m), 932 (m), 758 (m), 730 (m), 690 (s) cm^{-1}.

^{1}H NMR data (CD_2Cl_2, −55 °C, δ relative to Me_4Si): δ 2.96 (s, 3 H, NMe_2), 3.16 (s, 3 H, NMe_2), 3.50 (s, 6 H, NMe_2), 3.91 (s, 6 H, NMe_2), 4.43 (d, J = 8 Hz, 1 H, C_6H_5), 5.99 (t, J = 7 Hz, 1 H, C_6H_5), 6.36 (m, 2 H, C_6H_5), 6.56 (t, J = 6 Hz, 2 H, NC_5H_5), 7.07 (m, 2 H, NC_5H_5 and C_6H_5 superimposed), 7.36 (t, J = 6 Hz, 2 H, NC_5H_5), 7.46 (t, J = 6.1 Hz, 2 H, NC_5H_5), 9.26 (d, J = 5.9 Hz, 2 H, NC_5H_5), 9.75 (s, 1 H, $PhC_2\mathit{H}$).

$W_2Cl_4(NMe_2)_2(\mu$-$C_2Me_2)(py)_2$. $W_2Cl_2(NMe_2)_4(\mu\text{-}C_2Me_2)(py)_2\cdot py$ was prepared as described earlier. A 0.45-g sample of this compound was dissolved in toluene (5 mL) and stirred at ca. 55 °C for a period of 12 h. The blue-green solution turned yellow-brown with the formation of a yellow precipitate, which was collected by filtration and washed with toluene (5 mL). This yellow solid was redissolved in pyridine (5 mL) and layered with hexane. Orange-green crystals of $W_2Cl_4(NMe_2)_2(\mu\text{-}C_2Me_2)(py)_2$ were isolated by filtration after 7 days; yield 0.10 g (51%) according to eq 6. Anal. Calcd for $W_2Cl_4N_2C_{18}H_{28}$: C, 26.7; H, 3.5; N, 6.9; Cl, 17.5. Found: C, 26.5; H, 3.4; N, 6.8; Cl, 17.3.

IR data (Nujol, CsI plates): 1605 (s), 1489 (s), 1350 (w), 1260 (w), 1215 (m), 1065 (w), 1040 (w), 1010 (s), 915 (w), 800 (w), 760 (s), 7209 (w), 700 (s), 630 (w), 295 (m) cm^{-1}.

^{1}H NMR data (CD_2Cl_2, 21 °C, δ relative to Me_4Si): δ 2.50 (s, 6 H, μ-C_2Me_2), 3.74 (s, 6 H, NMe_2), 4.25 (s, 6 H, NMe_2), 7.62 (t, J = 6 Hz, 4 H, NC_5H_5), 8.02 (t, J = 6.1 Hz, 2 H, NC_5H_5), 9.22 (d, J = 6 Hz, 4 H, NC_5H_5).

^{13}C NMR data (CD_2Cl_2, 21 °C, δ relative to Me_4Si): 213.5 (μ-C_2Me_2), 154.9, 140.2, 124.7 (NC_5H_5), 64.1, 57.0 (μ-NMe_2), 22.2 (μ-$C_2\mathit{Me}_2$).

Crystallographic Studies. General operating facilities and listings of programs have been given previously.[22] Crystal data for the three compounds studied in this work are summarized in Table X.

$W_2Cl_2(NMe_2)_4(\mu$-$C_2H_2)(py)_2\cdot CH_2Cl_2$. The sample used in the study was cleaved from a larger crystal and transferred to the goniostat by using standard inert-atmosphere handling techniques. A systematic search of a limited hemisphere of reciprocal space revealed a set of no systematic absences or symmetry, indicating a probable space group of $P\bar{1}$. The structure was solved by a combination of direct methods (MULTAN 78) and Fourier techniques and refined by full-matrix least squares. All hydrogen atoms were located and refined.

A final Fourier was featureless, the largest peaks being 0.65 and 0.59 e/Å^3, located adjacent to the two metal positions.

$W_2Cl_3(NMe_2)_3(\mu$-$PhC_2H)(py)_2\cdot{}^1/_2C_7H_8$. The crystal used in the study was cleaved from a conglomerate and transferred to the goniostat by using standard inert-atmosphere techniques. A systematic search of a limited hemisphere of reciprocal space yielded a set of reflections which exhibited monoclinic symmetry and systematic extinctions corresponding to the space group $P2_1/n$.

The structure was solved by using a combination of direct methods and standard heavy-atom Fourier techniques. The W atoms were located by using MULTAN, and the remaining atoms were located in a difference Fourier phased with the W atoms. A subsequent difference Fourier indicated the presence of a solvent molecule situated at a center of symmetry. The asymmetric unit contains one molecule of $W_2Cl_3(NMe_2)_3(\mu$-PhCCH)$(py)_2$ and one-half molecule of toluene. The crystal shape was quite irregular, and attempts at an absorption correction failed to improve the data. The hydrogen atoms were not located but were inserted in calculated positions and remained fixed during the least-squares refinements, where all other atoms were refined by using anisotropic thermal parameters. Attempts at locating the H atom on the acetylenic carbon atom failed (this H atom was omitted during refinements).

The final difference Fourier contained a few peaks of approximately 1.3 e/Å^3, they were located within 1.2 Å of the W atoms.

(22) Chisholm, M. H.; Folting, K.; Huffman, J. C.; Kirkpatrick, C. C. *Inorg. Chem.* **1984**, *23*, 1021.

$W_2Cl_4(NMe_2)_2(\mu$-$C_2Me_2)(py)_2$. A suitable crystal was cleaved from a larger mass and transferred to the goniostat by using standard inert-atmosphere handling techniques. It should be noted that there appeared to be two definite sizes of crystals present. The larger crystals (a fragment of which was used herein) were, in general, covered with a layer of much smaller diamond-shaped platelets. There was no evidence that the two forms were the same. The sample was cooled to −160 °C after transfer to the goniostat and characterized in the usual manner (space group $P2_1/n$, based on 24 close-in reflections).

The structure was solved by location of the tungsten atoms in a Patterson synthesis, followed by Fourier techniques. All atoms, including hydrogens, were located and refined (isotropic for H; anisotropic for W, N, and C). The hydrogen atoms, while qualitively correct, show a significant scatter from the idealized positions expected on the basis of normal sp^3 bonding. ψ scans indicated absorption to be a problem, and the data were corrected accordingly. The residual dropped from $R(F) = 0.065$ to 0.039 and $R_w(F) = 0.068$ to 0.041 after the absorption correction was applied.

A final difference Fourier revealed four peaks of magnitude 0.9–1.5 e/Å^3 within 0.3 Å of the two tungsten atoms, and no other features were present. It should be noted that the thermal ellipsoids for C(7)–C(10) are somewhat "misshaped". A difference Fourier phased on all atoms, excluding C(7)–C(10), failed to indicate any disorder. We assume the large anisotropic shape is an artifact of the absorption correction as opposed to a thermal and/or disorder problem.

Acknowledgment. We thank the National Science Foundation and the Wrubel Computing Center for financial support.

Registry No. I, 102614-66-4; II, 102614-67-5; III, 102630-04-6; IV, 96503-06-9; V, 102614-69-7; VI, 96503-07-0; $CH_3C{\equiv}CH$, 74-99-7; $PhC{\equiv}CH$, 536-74-3; $HC{\equiv}CH$, 74-86-2; $CH_3C{\equiv}CCH_3$, 503-17-3; W, 7440-33-7.

Supplementary Material Available: Tables of anisotropic thermal parameters and complete listings of bond distances and bond angles (5 pages); a listing of F_o and F_c (9 pages). Ordering information is given on any current masthead page. The complete structural reports are available in microfiche form only from the Indiana University Chemical Library at a cost of $2.50 per copy. Requires MSC Report No. 85005 for $W_2Cl_4(py)_2(NMe_2)_2(\mu$-$C_2Me_2)$, No. 84091 for $W_2Cl_3(NMe_2)_3(py)_2(\mu$-$PhC_2H)\cdot{}^1/_2C_7H_8$, and No. 85032 for $W_2Cl_2(NMe_2)_4(py)_2(\mu$-$C_2H_2)\cdot CH_2Cl_2$.

Stereoelectronic Causes of an Unusual Coordination Geometry of an Acetylene

Maria José Calhorda and Roald Hoffmann*

Department of Chemistry, Cornell University, Ithaca, New York 14853

Received January 14, 1986

The recently synthesized $W_2(\mu$-$NMe_2)(\mu$-$C_2Me_2)Cl_4(py)_2$ complex is unique in featuring an acetylene twisted relative to the W–W axis to a geometry intermediate between parallel and perpendicular. Extended Hückel calculations provide an explanation for this deformation. In the perpendicular geometry one finds a small HOMO–LUMO gap, one which suggests, by a second-order Jahn–Teller argument, a twisting. This is true even in a hypothetical symmetrical environment, such as the hexachloride. But the potential energy minimum for one of the two twisted minima is much deepened by the asymmetric substitution. This effect can be traced to one metal–acetylene bonding orbital and is the result of a specific acetylene–carbon–chloride repulsive secondary interaction.

Until recently the myriad known dinuclear acetylene transition-metal complexes have fallen into two distinct types: "perpendicular", 1, and "parallel", 2.[1] The distinction refers to the projected angle between the M–M

0276-7333/86/2305-2181$01.50/0